

# Three-Dimensional Analysis of Skeletal Muscle Tissue by Fluorescent Reporters

Smrithi Karthikeyan<sup>1,2,3</sup>, Yoko Asakura<sup>1,2,3</sup>, Mayank Verma<sup>1,2,3,4</sup>, Atsushi Asakura<sup>1,2,3</sup>

<sup>1</sup> Stem Cell Institute, University of Minnesota Medical School <sup>2</sup> Paul & Sheila Wellstone Muscular Dystrophy Center, University of Minnesota Medical School <sup>3</sup> Department of Neurology, University of Minnesota Medical School <sup>4</sup> Department of Pediatrics & Neurology, Division of Pediatric Neurology, The University of Texas Southwestern Medical Center

## Corresponding Author

Atsushi Asakura  
asakura@umn.edu

## Citation

Karthikeyan, S., Asakura, Y., Verma, M., Asakura, A. Three-Dimensional Analysis of Skeletal Muscle Tissue by Fluorescent Reporters. *J. Vis. Exp.* (), e65400, doi:10.3791/65400 (2023).

## Date Published

June 2, 2023

## DOI

10.3791/65400

## URL

jove.com/t/65400

## Abstract

As the most abundant type of tissue, skeletal muscle is a highly organized tissue composed of a complex network of diverse cells. During times of injury and disease, the dynamic interactions between cells in this network give the skeletal muscle its extraordinary regenerative ability. Imaging is one of the most powerful tools used to visualize/study the spatial interactions between cells, including muscle stem cells (satellite cells), during muscle development and regeneration. Traditionally, horizontal muscle cross sections are immunolabeled and examined underneath a conventional light microscope.

Although this method provides valuable information on the orientation of cells on a horizontal plane, the axial orientation of the cells is lost. This leads to an underrepresentation of the actual 3D orientation of different cells in a muscle section. Therefore, to understand the skeletal muscle cellular network accurately, one must gain information from all three dimensions (3D). Due to advances in imaging and computing technology, confocal microscopy is a powerful tool for analyzing spatial data. The use of an optimal optical clearing protocol enables the production of a more accurate 3D image of the muscle without the need for physical sectioning of the muscle.

This paper presents a new method for clearing skeletal muscle tissue and confocal image acquisition. The second part outlines a time-efficient protocol for computational analysis of confocal images and 3D rendering. Overall, the imaging techniques outlined would lead to 3D, whole-tissue quantification of a muscle section. This would allow for a better understanding of the spatial orientation and cross-cellular interactions between different cells in the skeletal muscle network during muscle homeostasis, injury, disease, and repair.

## Introduction

Skeletal muscle is a highly-ordered tissue that performs the following vital functions in the human body: breathing, posture maintenance, and voluntary locomotion. Unlike other body tissues, skeletal muscle can regenerate/adapt in response to various physiological demands, such as exercise and growth<sup>1</sup>. By composition, skeletal muscle is composed of a complex network of the following diverse variety of cells: multinucleated muscle fibers, muscle stem cells (also known as satellite cells), blood vessels, pericytes, fibroadipogenic progenitors (FAPs), mesenchymal progenitors, immune cells, and undefined fibroblastic cells<sup>2,3,4,5</sup>. The spatial orientation and interplay between these cells in the network change drastically from the basal state in times of development, injury, and disease. Therefore, understanding the structure, function, and orientation of cells within the skeletal muscle network during times of homeostasis, injury, and disease is critical to providing a more holistic understanding of the regeneration process. A clearer understanding of this process would in turn provide new insights into various neurodegenerative diseases, such as Duchenne muscular dystrophy (DMD)<sup>6</sup>.

Imaging is one of the most powerful techniques to study the spatial interaction of cells in the skeletal muscle network. Conventionally, the skeletal muscle cellular network has been analyzed two-dimensionally *via* muscle cross sections. These cross sections are typically obtained from frozen or paraffin-embedded tissue blocks, which are then immunolabeled to differentiate the different cell types. Following immunolabeling, a single slice is examined under a light microscope. While this method is useful for providing information on the cellular interactions on a lateral plane, information in the axial direction is completely lost, leading

to a misrepresentation of the 3D network. As cells in the network interact with each other in a 3D way, it is important that the method of analysis obtains information from all three dimensions<sup>4,7</sup>.

One method of 3D studying the spatial interaction of cells is to image a series of cross sections. After imaging, a 3D model of the muscle is reconstructed, compiling the individual images manually or automatically. However, this process is labor-intensive and error-prone, as various unwanted artifacts can be present in each cross section. Another method of 3D imaging is optical sectioning, which uses confocal microscopy and software deconvolution to provide a 3D representation of a muscle sample. In previous protocols, this method has been severely limited by the presence of light-scattering molecules, such as lipids, and endogenously fluorescent molecules (myoglobin and NADH). However, this problem can be addressed by utilizing a protocol that would reduce the light-scattering effects *via* refractive index mismatching while preserving the original fluorescence from the importer molecule. This paper proposes an ideal optical tissue-clearing protocol, a confocal image acquisition method, and 3D rendering of the muscle section image<sup>7</sup>.

## Protocol

**NOTE:** Before perfusion fixation, *Pax7<sup>tdTomato</sup>:Flk1<sup>GFP</sup>* mice were injected with tamoxifen as previously described<sup>4</sup>. *Pax7<sup>tdTomato</sup>:Flk1<sup>GFP</sup>* (*Pax7<sup>+/CreERT2</sup>:R26R(het):Flk1<sup>+/GFP</sup>*) mice were generated *via* breeding *Pax7<sup>+/CreERT2</sup>*, *R26R(het)*, and *Flk1<sup>+/GFP</sup>* mice, as shown in **Table of Materials**. During imaging, the vasculature appeared as green (expressing the GFP protein from *Flk1<sup>+/GFP</sup>*) and the satellite cells appeared as red (expressing the tdTomato

protein from *Pax7<sup>tdTomato</sup>*). The overall workflow of this protocol is schematically shown in **Figure 1**. Tamoxifen was dissolved in corn oil at a concentration of 20 mg/mL by shaking overnight at 37 °C, and the aliquots were stored in a -80 °C freezer. A dose of 75 mg of tamoxifen per kilogram body weight was intraperitoneally (i.p) injected into mice for 2 consecutive days. All animal studies were approved by the IACUC at the University of Minnesota (2204A39969). The **Table of Materials** provides details related to all materials, software, instruments, and reagents used in this protocol.

## 1. Perfusion fixation and dissection **Figure 2A ,B)**

1. Use isoflurane inhalant anesthesia (3%-4% for induction and 1%-3% for maintenance) for the mice, as previously described<sup>4</sup>. Pin the mouse on a fixation chamber.
2. Use sterilizing solution (betadine, hibiclens, or novalson) for skin preparation prior to surgery. Expose the heart by opening the chest cavity and pin the ribs up. Insert and secure the needle (25 G) into the left ventricle of the heart and connect the needle to the tube for a syringe pump (**Figure 2A**). It is required to make an incision in the right atrium for the blood and buffer solutions to flow out.  
<sup>^ Space is needed here</sup>
3. Perfuse with 5 mL of phosphate-buffered saline (PBS) with a 2 mL/min flow speed, followed by 50 mL of fixation buffer (**Table 1**) with 2 mL/min flow speed.  
**NOTE:** Movement of mouse's tail during this process indicates that the perfusion has been done well. It is important that the heart is beating at the beginning of this process for the PBS to flow into the muscles properly.
4. Detach the extensor digitorum longus (EDL) muscle as follows (**Figure 2B**): carefully lift the EDL tendon end next to the tibialis anterior (TA) tendon with forceps and cut

as close to the foot as possible. Release the EDL muscle from the other muscles until the upper tendon is visible, then sever the upper tendon.  
<sup>^ (Figure 1B)</sup>

5. Postfix the tissues with fixation buffer (10 mL per two EDL muscles) in a 15 mL conical tube at 4 °C with rocking overnight.
6. Wash with 10 mL of ice-cold PBS + 0.02% sodium azide (NaN<sub>3</sub>) 3x 30 min at 4 °C with rocking.

Change the correct font size

## 2. Tissue clearing

1. Thaw A4P0 solution (**Table 1**) on ice. Ensure that the temperature of the solution remains around 4 °C.
2. Transfer 10 mL of A4P0 into a 15 mL plastic tube with the muscle.
3. Incubate the muscle in cold A4P0 (10 mL) overnight at 4 °C with rocking.
4. The next day, thaw and transfer 10 mL of A4P0 into a 50 mL plastic tube.
5. Degas the A4P0 solution on ice by bubble nitrogen gas for 3 min.
6. Allow the solution to settle so that the bubbles in the solution are gone.  
**NOTE:** This should happen in approximately 1 min.
7. Remove the A4P0 solution from the tube and collect the waste for proper disposal.
8. Transfer the "degassed" A4P0 from the 50 mL tube into the 2 mL tube containing the sample. Overfill the tube until a meniscus forms but do not allow air bubbles to form inside the tube.
9. Lightly cover the tube with 1 inch x 1 inch plastic wrap so as not to introduce any air bubbles.

10. Screw the cap on top of the tube tightly; allow excess liquid to drip down into waste.
11. Incubate the samples at 37 °C in a tube rotator to polymerize the A4P0. Allow polymerization for 3 h in a tube wrapped in aluminum foil.
12. Remove the tissue from the A4P0 solution and discard the waste appropriately.
13. Wash with 10 mL of PBSTT (**Table 1**) 3 x 30 min at 37 °C.
14. Transfer the samples to the 10 mL clearing solution 1 (CS1) (**Table 1**) overnight at 37 °C with rocking.  
**NOTE:** The EDL muscles are left overnight.
15. Wash 3 x 30 min with PBSTT (10 mL) with rocking at 37 °C.
16. Incubate the tissue in 10 mL of clearing solution 2 (CS2) (**Table 1**) overnight at 37 °C with rocking. After overnight incubation, the tissue now appears clear.
17. Wash 3 x 30 min with PBSTT (10 mL) with rocking at 37 °C.
18. Incubate the EDL muscle in 10 mL of PROTOS 3 x 30 min at 37 °C with rocking.
19. Use the PROTOS solution and the embedding method to perform multiview imaging described below.
20. Store the samples in PROTOS after imaging at 4 °C.

### 3. Embedding (Figure 2C-E)

1. Press an approximately 1 inch piece of tape to one side of the silicon isolator to remove any dust particles. Use a silicon isolator (1.6 or 2.4 mm depth, dependent on the EDL muscle size; see **Table of Materials**) for tissue mounting, as shown in **Figure 2C**.

2. Attach the clean side of the isolator to the center of a cover glass by firmly pressing the spacer to the glass.
3. Press another piece of tape to the exposed side of the isolator to clean off any remaining dust particles.
4. Place the sample (which was in the PROTOS solution) into the isolator using tweezers (Dumont #5).
5. Fill the isolator with the remaining PROTOS solution with a pipette until the muscle sample is submerged in the isolator.
6. Attach the top cover glass by pressing it onto the spacer/glass complex below.  
**NOTE:** Make sure there are no bubbles in the isolator.

### 4. Image acquisition

**NOTE:** A confocal microscope is required to image the cleared tissue samples. Images of the skeletal muscles' vasculature and satellite cells were taken using green fluorescent protein (GFP) and mCherry filters (mCherry has a similar excitation/emission maxim as tdTomato).

1. Key parameters for image acquisition
  1. Switch on the **488 nm (GFP)** and **561 nm (mCherry)** lasers on the laser controller.  
**NOTE:** The vascular endothelial cells expressing GFP are detected by the 488 nm (GFP) channel, and the satellite cells expressing tdTomato are detected by the 561 nm (mCherry) channel.
  2. Ensure that the pinhole diameter for the **shortest wavelength laser** (the **488 nm** laser) is **1.2 µm**. Adjust it in the **A1 Compact GUI** window.  
**NOTE:** A pinhole size of 1.2 µm is the optimal size to allow enough light to the detector to see the sample with the highest resolution (good clarity of all signals).

without completely bleaching out the sample). A pinhole size of up to 1.5  $\mu\text{m}$  can be used.

3. Select an image size of **1024 x 1024 pixels** in the **A1 Compact GUI** window.
4. Select a **Z range of 400  $\mu\text{m}$  (401 steps)** in the **Scanning Window**.
2. General protocol for image acquisition
  1. Turn on the confocal microscope based on the facility/manufacture's instructions. Ensure the **488 nm** and **561 nm** lasers are turned on ~~on~~ **at** the **laser controller**.
  2. Select the **20x** water immersion objective lens of the microscope. Place two or three drops of distilled water onto the lens using a syringe.
  3. Place the embedded sample slide onto the stage.
  4. In the NIS Elements software, select the **Eyepiece-EPI** tab in order to be able to find the sample using the eyepiece of the microscope. Select **mCherry** or **GFP** in the menu to switch on the **laser** of the corresponding wavelength.
  5. At the microscope, find an area in the sample in which satellite cells are visible in mCherry and blood vessels are visible in GFP.
  6. Move the laser strength slider for each laser (mCherry and GFP) in the **A1 Compact GUI** window to adjust the image **brightness** in both channels so that very few spots of the image are saturated.
  7. As the sample is 3D, identify the top and the bottom of the sample for the microscope to take the image. Adjust the **Z** position using the side knobs of the microscope until the top of the sample is reached.

8. When the top of the sample is reached, click **Top** in the **Scanning Window**. Manually enter the corresponding bottom to ensure the image's total depth is **400  $\mu\text{m}$** .
9. In the **A1 Compact GUI** window, select the desired image size of the **1024 pixel scan area**.
10. Click **Run Now** in the **Scanning Window** to take the image and wait for a new window to pop up displaying the image acquisition time.
11. After the images have been taken, Click **File | Save As** to save the image in a desired location in **ND2 file format**.
12. To convert the image file to a **TIF/TIFF format** for analysis, open the ND2 file in FIJI ImageJ (9, 10). Once opened, select **File | Save As | Tiff**.

## 5. Image segmentation/analysis (Figure 3)

**NOTE:** The overall process of 3D rendering a microscope image involves segmenting the original microscope image using the software ilastik and then creating a 3D render with Imaris. Segmentation converts an image into a binary image. Different segmentation software applications have been developed; this protocol uses ilastik for its ease of use and powerful segmentation algorithm<sup>11</sup>. After segmentation is complete, the segmented binary image can then be 3D rendered/analyzed through the visualization software Imaris.

1. General protocol for image segmentation using FIJI ImageJ and ilastik
  1. Import the raw image file (.nd2 file type) into FIJI ImageJ. Convert and save the image as a **TIF/TIFF** file type by clicking on **File | Save As | Tiff**.

2. For multichannel images, split the image channels of the TIF file by clicking on **Image | Color | Split Channels**.
3. Using the HDF5 plugin, save each channel in **HDF5** format by clicking on **File | Save As | HDF5 | Save to HDF5 (new or replace)**.
4. To ease the computational load of the ilastik software, crop the large image files into smaller images. For a 1024 x 1024 x 401 pixel image size (used in this protocol), crop parts of the image before loading into ilastik.
  1. In Fiji, click on **Image | Crop** and use the **rectangle cropping tool** from the toolbar. Crop at least five different **50 x 50 x 401 pixel images** from each channel.
5. Save each cropped image in **HDF5** file format (same protocol as step 5.1.3).
6. In ilastik, start a new **Pixel Classification** project file.
7. Open all the cropped image files (all .h5 file types) in the **Input Data** tab by clicking on **Add New | Add Separate Image(s)**.
8. In the **Feature Selection** tab, select all the available features by clicking on the **Select Features tab** and checking all of the boxes (to achieve this, drag the mouse over the boxes).
9. In the **Training** tab, create two labels. Designate one label as the **background** and define the other as the **feature of interest**.
 

**NOTE:** In this protocol, the feature of interest was either the satellite cells or the blood vessels.
10. After selecting a starting label (either background or feature of interest), select the **paintbrush tool** and identify the parts of the image that are either the background or the feature of interest. After identifying some spots, press **Live Update** with only the **Segmentation box** checked and observed the segmented version of the cropped image. Repeat this step until the segmentation is as accurate as possible.
11. Repeat step 5.1.10 for each cropped image.
12. In the **Prediction Export** tab, change the **Source** to **Simple Segmentation**.
13. In the **Batch Processing** tab, select the complete .h5 file of one of the channels of the original image by clicking the **Select Raw Data Files** button. Then, to segment the entire channel, click **Process all Files**.
14. Once the segmentation is complete, open the completed segmentation file in FIJI ImageJ by clicking **Plugins | ilastik | Import HDF5**.
15. Save the opened image in the **TIFF** file format.
16. If the TIFF image appears as black, in ImageJ, click on **Image | Adjust | Brightness | Contrast | Auto**. Make sure the image is not a virtual stack [denoted as (V)]. If so, the image must be reopened as a plain **TIFF** file.
17. To convert the image to binary, adjust the thresholding by clicking on **Image | Adjust | Threshold | Auto | Apply** and uncheck **Calculate Threshold for each Image**.
18. Repeat steps 5.1.4-5.1.17 for each channel of the original image. With multichannel images, after



individual segmentation, merge the channels again on FIJI by clicking on **Image | Color | Merge Channels**. Optional: click the **Look Up Table** option (LUT) in Fiji's toolbar to give each channel a different color for labeling purposes.

19. Save the merged image as a TIFF file.

## 2. General protocol for 3D rendering and data collection using Imaris

1. To be able to open up the segmented image in Imaris, convert the TIFF file into an Imaris file using the Imaris file converter (which is given with the Imaris software package).

2. In Imaris, make sure the following licenses are selected: **Imaris Cell**, all of the **MeasurementPro** options, and **Imaris XT**. The MeasurementPro options allow the computer to take measurements in multichannel images.

3. In the **Surpass** tab, open up the merged image file (now an Imaris file).

4. In the **Scene** tab, create a surface (by clicking on the **blue icon**). Create the same number of surfaces as the number of channels in the image. Each surface represents a different feature of interest.

**NOTE:** In this case, one surface represents muscle satellite cells, and the other represents blood vessels.

5. In the **Surfaces** tool, ensure the **Object-to-Object Statistics** and **Background Subtraction** boxes are checked. Uncheck the **Classify Surfaces** box. Do this for each surface in the multichannel image.

6. Press the **green arrows** to continue and create a 3D-rendered surface of the feature of interest.

7. To collect data between the two surfaces, click the **Statistics** tab to get several measurements of the surfaces (including **Volume**, **Density**, **Shortest Distance to other Surfaces**, and **Sphericity**) in the **Detailed Specific Values** tab. Save all data points collected as a .csv file and open them in a spreadsheet for further data analysis.

## Representative Results

After tissue clearing (**Figure 2**), the EDL muscle sample is imaged using a confocal microscope. As can be seen in **Figure 3A**, the blood vessels appear green in the confocal image due to the GFP protein present in the skeletal muscle sample<sup>12</sup>. In **Figure 3B**, the satellite cells appear as bright red spots in the confocal image due to the presence of the tdTomato protein in muscle stem cells. Upon closer inspection of **Figure 3**, the myofibers display a faint red background fluorescence in the confocal image. As the mice selected in this sample are *mdx* mice, the satellite cells undergo constant renewal and regeneration to repair the muscle fibers<sup>13</sup>. However, as the *mdx* mice muscles undergo constant repair, some of the satellite cells undergo a differentiation process and fuse with a muscle fiber to repair the fiber. Some myofibers appear red as the *tdTomato* gene is still expressed. The background red can be removed completely during the image segmentation process in ilastik. After the 3D model is generated (**Figure 3C,D**), the following parameters can be measured in Imaris using the model: satellite cell sphericity (used as a measure of the satellite cell's shape; **Figure 4A**), satellite cell volume (**Figure 4B**), and the distance between the satellite cells and the vasculature (**Figure 4C**). In addition, the parameters for tortuosity of the vasculature and blood vessel density can be measured in Imaris (data not shown).

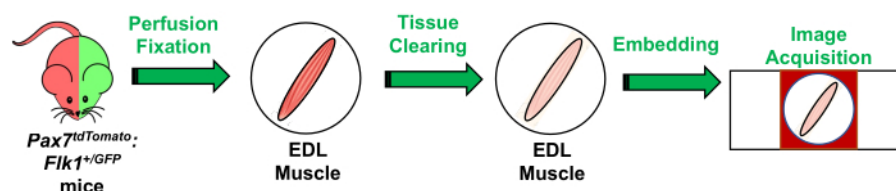


**Figure 1: Overall workflow diagram for 3D imaging from an EDL muscle sample.** *Pax7<sup>tdTomato</sup>:Flk1<sup>GFP</sup>* mice were used for perfusion fixation. The EDL muscle was dissected and tissue clearing was performed. The cleared EDL muscle was embedded into the silicon isolator with cover glasses for image acquisition. Abbreviations: GFP = green fluorescent protein; EDL = extensor digitorum longus. [Please click here to view a larger version of this figure.](#)

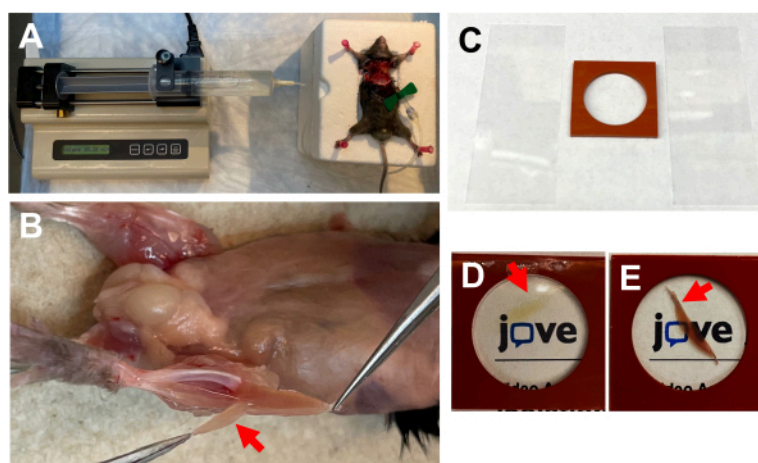


**Figure 2: Dissection of the EDL muscle.** (A) *Pax7<sup>tdTomato</sup>:Flk1<sup>GFP</sup>* mice received tamoxifen and were used for perfusion fixation by a syringe pump after anesthetization. (B) After perfusion fixation and removal of the skin, the EDL muscle (red arrow) was separated from the other hindlimb muscles. (C) A silicone isolator with a pair of cover glasses was used for image acquisition. (D) Following tissue clearing, the EDL muscle became transparent, and the letters below the EDL muscle were clearly visible. (E) Without tissue clearing, the EDL muscle was dark and covered the letters below the muscle. Abbreviations: GFP = green fluorescent protein; EDL = extensor digitorum longus. [Please click here to view a larger version of this figure.](#)



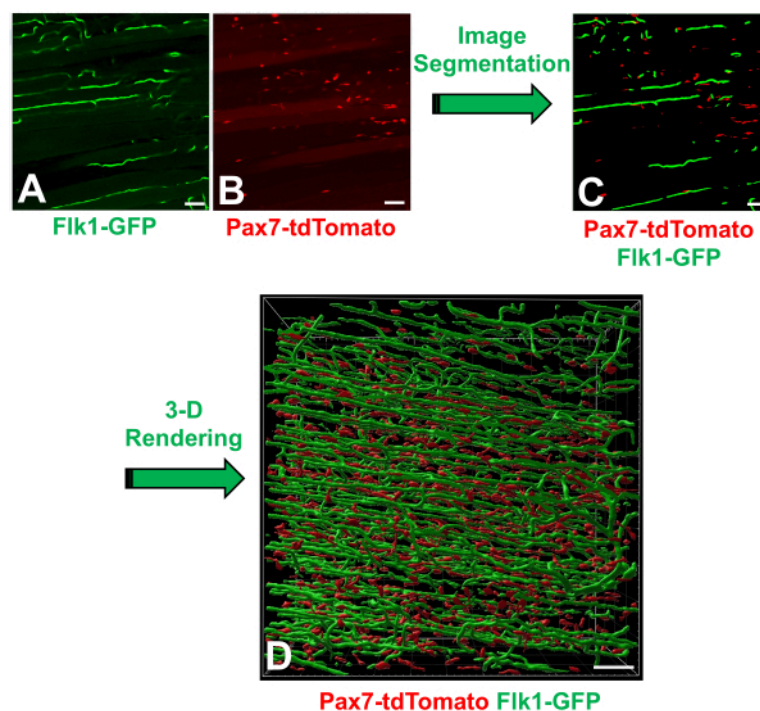


**Figure 3: Image of the 3D rendering process of an *mdx* mouse EDL muscle sample.** *Pax7<sup>tdTomato</sup>:Flk1<sup>GFP</sup>* (*Pax7<sup>+/+</sup> CreERT2<sup>-/-</sup>:R26R(het):Flk1<sup>+/GFP</sup>*) mice were used for the 3D imaging analysis. (A) Blood vessel confocal image (Flk1-GFP). (B) Satellite cell confocal image (Pax7-tdTomato). (C) Segmented image with both blood vessels and satellite cells (Flk1-GFP, Pax7-tdTomato). (D) A 3D rendering image of an EDL muscle sample (Flk1-GFP, Pax7-tdTomato). Abbreviations: GFP = green fluorescent protein; EDL = extensor digitorum longus. Scale bars = 20  $\mu$ m. [Please click here to view a larger version of this figure.](#)

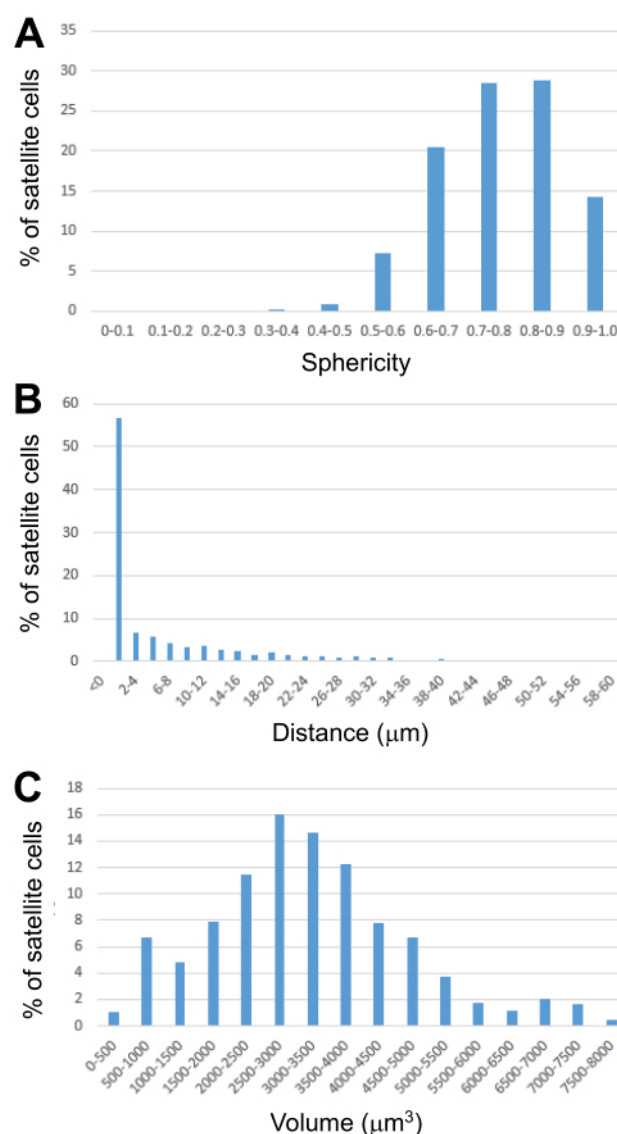


**Figure 4: Parameter measurements from the 3D model in Figure 1D.** (A) Percent (%) distribution of satellite cell sphericity. (B) Percent (%) distribution of the distance between individual satellite cells and the vasculature. (C) Percent (%) distribution of satellite cell volume. [Please click here to view a larger version of this figure.](#)

#### Table 1: Composition of solutions used in this protocol.

[Please click here to download this Table.](#)

## Discussion

*In situ* real-time imaging is an excellent tool for analyzing organelles within a cell. To grasp a better picture of how

different cells interact with each other within a muscle, the approach shown in this study would be ideal. In this protocol, satellite cells and blood vessels can be analyzed in a 3D manner through confocal microscopy.

To analyze the muscle section in the confocal microscope, the tissue section must undergo the perfusion fixation process and then be optically cleared. Overall, the perfusion fixation and tissue clearing protocol take approximately 5 days to complete. For an EDL muscle sample, the image acquisition step takes approximately 1 h to complete. For proper image acquisition, in order to select the ideal confocal microscope lens, the working distance of the lens and the thickness/size of the muscle sample must be known. For EDL tissue-cleared muscles, the 20x water immersion lens on the microscope used here provides precise results. Usually, water immersion lenses provide more transparent images for two-photon confocal imaging. Image segmentation and 3D rendering of the confocal image take ~2 h to complete per image. Although this method is time-consuming, it produces the most accurate 3D representation of the cellular network present within the skeletal muscle. Another method of analyzing the skeletal muscle in 3D is to image a series of longitudinal sections. Later, the images can be manually/automatically merged to generate the 3D image<sup>7</sup>. However, this process is more error-intensive and error-prone due to the presence of artifacts in the cross sections.

The method provided in this study does not physically cut through the muscle, providing a more accurate representation in the 3D model. In addition, this method is flexible and can be applied to any other type of cell in the muscle. The signal level obtained with conventional confocal microscopy rapidly decreases with depth, even when the refractive indices of the sample and the immersion medium are matched, due to the discontinuities in the refractive index within biological tissue, causing light scattering. Multiphoton microscopy is capable of imaging to more than twice the depth of confocal microscopy and is generally considered the best method for imaging deep tissue. However, multiphoton microscopy is also ultimately

limited by scattering. Against this background, our clearing techniques have been established for deep muscle imaging of highly scattering tissues.

Some critical steps of the above method are the following: when adding the fixation buffer, it is important only to add the buffer while the heart is still beating so the buffer can flow into the muscles properly. Further, if the fixation is done successfully, the mouse's tail should move during the process. During tissue clearing, it is necessary to maintain appropriate incubation times and temperatures for each step of the process. In addition, since the thickness of the EDL muscle is different, two types of isolators, 2.4 mm and 1.6 mm, are available, and better 3D imaging results can be obtained by using isolators of a slightly thicker size than the EDL muscle.

During the image acquisition steps (protocol section 4), one common mistake is that the image layers do not appear to change in the scanning window. If this occurs, it is indicative that the sample has the lens of the microscope. To avoid this error, it is important that the scientist runs through all 401 layers before taking the image by just turning the Z-axis wheel to ensure the sample is thick enough without hitting the microscope lens. In addition, during the last steps of image segmentation (protocol step 5.1.19), another common pitfall is that the two segmented channels (blood vessels and satellite cells) can be merged incorrectly. Sometimes, the ilastik software can mirror the binary image/rotate the binary image by 180°. If left unnoticed, the possibility of incorrectly merging the segmented channels exists. If one channel is rotated, one workaround is to rotate the channel back using the following commands in Fiji: **Image | Transform | Rotate**.

A limitation of this protocol is that, especially in *mdx* mice, there is a high background from the tdTomato muscle fibers

(**Figure 3B**). In *mdx* mice, the skeletal muscle cells undergo constant regeneration even under normal conditions (not under exercise or stress)<sup>13</sup>. Therefore, when the muscle undergoes regeneration, the tdTomato-expressing satellite cells undergo differentiation/proliferation and fuse with the muscle fiber to repair. This leads to the muscle fiber appearing red, making it more difficult to focus purely on analyzing the satellite cells. To overcome this problem, the time between tamoxifen injection and confocal imaging of the muscle fibers can be reduced from 1 month to a couple of days. In addition, the background can be eliminated through careful segmentation in ilastik. **If both methods are done, and there is still significant background, a careful filter in Imaris during the 3D rendering can be done.** Muscle satellite cells have a characteristic star/spindle shape with 10-20  $\mu\text{m}$  diameters<sup>14</sup>. During 3D rendering, if some objects display an atypical size (such as volumes that are considerably smaller or larger by a fivefold magnitude than what the typical satellite cell would be), these objects can be deselected, only leaving behind the actual size of the satellite cell. The main challenge is that the large file sizes make the image segmentation process take close to ~~3 h~~<sup>hours</sup> for ilastik to train. The expected file size for the image should be 1,644,368 KB.

This optical tissue clearing protocol is applicable to immunostained muscle tissue, such as using anti-laminin antibody after whole-mount immunostaining<sup>7</sup>. However, the sensitivity and high background of whole-mount immunostaining limit the antibodies that can be used. An example of the importance of 3D imaging is the documentation of the interaction between muscle satellite cells and endothelial cells. Satellite cells preferentially locate themselves near blood vessel endothelial cells *via* vascular endothelial growth factor (VEGF) and Notch signaling<sup>4,5,15</sup>. Currently, the protocol has been utilized for other skeletal

muscle models such as aging, injured, and satellite cell-ablated muscles, and has provided similar tissue clearing results. Using the data from the 3D-rendered image, new insights can be found when looking at the skeletal muscle cellular network and various neurodegenerative diseases such as DMD.

**Highlighted Reword: "If there is a significant background after attempting both methods, background objects can be filtered out in Imaris during 3D rendering."**

## Disclosures

The authors have no conflicts of interest to declare.

## Acknowledgments

We thank the Minnesota Supercomputing Institute (MSI) and the University of Minnesota Imaging Center (UIC). We also thank Jake Trask for the critical reading of this paper. This work was supported by NIH R01AR062142, NIH R21AR070319, and a Regenerative Medicine Minnesota (RMM) Grant to AA.

## References

- Schmidt, M., Schüler, S. C., Hüttner, S. S., von Eyss, B., von Maltzahn, J. Adult stem cells at work: regenerating skeletal muscle. *Cellular and Molecular Life Sciences*. **76** (13), 2559-2570 (2019).
- Asakura, A., Komaki, M., Rudnicki, M. Muscle satellite cells are multipotential stem cells that exhibit myogenic, osteogenic, and adipogenic differentiation. *Differentiation*. **68** (4-5), 245-253 (2001).
- Asakura, A., Seale, P., Girgis-Gabardo, A., Rudnicki, M. A. Myogenic specification of side population cells in skeletal muscle. *The Journal of Cell Biology*. **159** (1), 123-134 (2002).

4. Verma, M. Muscle satellite cell cross-talk with a vascular niche maintains quiescence via VEGF and Notch signaling. *Cell Stem Cell*. **23** (4), 530-543.e9 (2018).
5. Relaix, F. et al. Perspectives on skeletal muscle stem cells. *Nature Communications*. **12** (1), 692 (2021).
6. Podkalicka, P., Mucha, O., Dulak, J., Loboda, A. Targeting angiogenesis in Duchenne muscular dystrophy. *Cellular and Molecular Life Sciences*. **76** (8), 1507-1528 (2019).
7. Verma, M., Murkonda, B. S., Asakura, Y., Asakura, A. Skeletal muscle tissue clearing for LacZ and fluorescent reporters, and immunofluorescence staining. *Methods in Molecular Biology*. **1460**, 129-140 (2016).
8. Chung, K., Deisseroth, K. CLARITY for mapping the nervous system. *Nature Methods*. **10** (6), 508-513 (2013).
9. Schindelin, J. et al. Fiji: an open-source platform for biological-image analysis. *Nature Methods*. **9** (7), 676-682 (2012).
10. Rueden, C. T. ImageJ2: ImageJ for the next generation of scientific image data. *BMC Bioinformatics*. **18** (1), 529 (2017).
11. Berg, S. et al. ilastik: interactive machine learning for (bio)image analysis. *Nature Methods*. **16** (12), 1226-1232 (2019).
12. Feng, X., Naz, F., Juan, A. H., Dell'Orso, S., Sartorelli, V. Identification of skeletal muscle satellite cells by immunofluorescence with Pax7 and laminin antibodies. *Journal of Visualized Experiments*. **134**, 57212 (2018).
13. Latroche, C. Structural and functional alterations of skeletal muscle microvasculature in dystrophin-deficient mdx mice. *The American Journal of Pathology*. **185** (9), 2482-2494 (2015).
14. Yin, H., Price, F., Rudnicki, M. A. Satellite cells and the muscle stem cell niche. *Physiological Reviews*. **93** (1), 23-67 (2013).
15. Den Hartog, L., Asakura, A. Implications of Notch signaling in Duchenne muscular dystrophy. *Frontiers in Physiology*. **13**, 984373 (2022).